Laser Chem., Vol. 13, pp. 187–205
Reprints available directly from the Publisher
Photocopying permitted by license only

THE SPECTROSCOPY AND PHOTOPHYSICS OF π HYDROGEN-BONDED COMPLEXES: BENZENE–$CHCl_3$

ALBERT J. GOTCH, R. NATHAN PRIBBLE, FREDERICK A. ENSMINGER, and TIMOTHY S. ZWIER*

Department of Chemistry, Purdue University West Lafayette, IN 47907–1393

(Received 10 March 1993)

A vibronic level study of the spectroscopy and photophysics of the C_6H_6–$CHCl_3$ complex has been carried out using a combination of laser-induced fluorescence and resonant two-photon ionization (R2PI). In C_6H_6–$CHCl_3$, the S_1–S_0 origin remains forbidden while the 16^1_0 transition is weakly induced. Neither 6^1_0 nor 16^1_0 are split by the presence of the $CHCl_3$ molecule. On this basis, a C_{3v} structure is deduced for the complex, placing $CHCl_3$ on the six-fold axis of benzene. The large blue-shift of the complex's absorption relative to benzene (+178 cm^{-1}) and the efficient fragmentation of the complex following one-color R2PI reflect a hydrogen-bonded orientation for $CHCl_3$ relative to benzene's π cloud. Dispersed fluorescence scans place a firm upper bound on the ground state binding energy of the complex of 2,024 cm^{-1}. Both the 6^1 and 6^11^1 levels do not dissociate on the time-scale of the S_1 fluorescence and show evidence of extensive state mixing with van der Waals' levels primarily built on the 0^0 level of benzene. The C_6H_6–$(CHCl_3)_2$ cluster shows extensive intermolecular structure beginning at +84 cm^{-1}, a strong origin transition, and splitting of 6^1. A structure which places both $CHCl_3$ molecules on the same side of the benzene ring is suggested on this basis. The vibronic level scheme used to deduce the structure of C_6H_6–$CHCl_3$ is tested against previous data on other C_6H_6–X complexes. The scheme is found to be capable, in favorable cases, of deducing the structures of C_6H_6–X complexes based purely on vibronic level data. Finally, the results on C_6H_6–$CHCl_3$ are compared with those on C_6H_6–HCl and C_6H_6–H_2O to evaluate the characteristics of the π hydrogen bond.

KEY WORDS: Vibronic spectroscopy, Cluster, Hydrogen bond

I. INTRODUCTION

Benzene's role as prototypical aromatic invites fundamental studies of its intermolecular interactions with various solvents. One approach to such studies focuses on the spectroscopy of the cold, gas phase benzene–X_n clusters formed in a supersonic expansion. These studies have in favorable cases provided information on the lowest energy benzene-solvent structures, bracketed their binding energies, made some headway in assigning intermolecular vibrations which characterize the intermolecular potential energy surface, and probed the nature and extent of

* Author to whom correspondence should be addressed.
Submitted to the Laser Chemistry special issue in honor of Mitsuo Ito.

intramolecular–intermolecular vibrational state mixing as a function of energy and vibrational mode. Recent years have seen cluster-size specific studies of benzene complexed to rare gas atoms,[1–7] N_2,[8] CO,[8] CO_2,[8] simple hydrocarbons,[9,10] CCl_4,[11] HCl,[12,13] H_2O,[14,15] CH_3OH,[16] and H_2O/CH_3OH mixtures.[17]

One of the intriguing aspects of the studies of benzene–HCl, $-H_2O$, and $-CH_3OH$ is the insight they provide to the pseudo-hydrogen bonding of these protic solvents to benzene's electron-rich π cloud. By contrast to the conventional linear X···HY hydrogen bond, the benzene···HY interactions involve delocalized electrons spread out over benzene's carbon framework.[18]

In this paper we extend our study of benzene complexes with hydrogen bonding solvents to include $CHCl_3$. Studies of benzene/chloroform solutions using n.m.r.,[19] infrared,[20] and Raman[20] spectroscopies have pointed toward the formation of a hydrogen-bonded C_6H_6–$CHCl_3$ complex in solution. Here we characterize the gas-phase C_6H_6–$CHCl_3$ complex by the perturbations imposed on the $S_1 \leftarrow S_0$ spectrum of benzene by the $CHCl_3$ molecule. From the symmetries of the vibrational fundamentals which gain intensity upon complexation, a C_{3v} geometry is deduced for the 1 : 1 complex. In the process of this study we have generalized a scheme for deducing vibrationally-averaged structures for C_6H_6–X complexes based solely on vibronic level symmetry arguments. We apply this scheme to the C_6H_6–X complexes studied by our group to date. A comparison of the structures and spectroscopy of C_6H_6–HCl, C_6H_6–H_2O, and C_6H_6–$CHCl_3$ provides some insight to the nature of the π hydrogen bond.

II. EXPERIMENTAL

The molecular beam time-of-flight mass spectrometer used in these studies has been described previously.[14] C_6H_6–$(CHCl_3)_n$ clusters are formed by expanding a mixture containing C_6H_6 and $CHCl_3$ in helium from a pulsed valve of 0.8 mm diameter operating at 20 Hz. The concentrations of these vapors are controlled by metering flows of helium over the room temperature liquids using needle valves and mixing these flows with the main flow of helium. Typical expansion conditions employ ~0.5% C_6H_6 and 0.1–1.0% $CHCl_3$ at a total pressure of 2–4 bar. The clusters are resonantly ionized by the unfocused output of an excimer-pumped dye laser operating on Coumarin 503, doubled in a β-barium borate crystal. Typical energies of 0.1–1.0 mJ/pulse are used. Mass-selected R2PI scans are recorded in the linear mode of the TOF mass spectrometer using a 100 MHz digital oscilloscope.

Fluorescence excitation scans, dispersed fluorescence scans, and fluorescence lifetime measurements are recorded in a second apparatus which has also been described elsewhere.[21] An excimer-pumped dye laser is used as excitation source at typical energies of 0.01–0.1 mJ/pulse. A 3/4-meter monochromator is used to record dispersed fluorescence scans at a resolution of about 40 cm^{-1} FWHM. Fluorescence lifetime measurements are 500 shot averages employing a 100 MHz digital oscilloscope.

III. RESULTS AND ANALYSIS

A. Vibronic Probes of Cluster Structure in C_6H_6–X complexes

In several previous studies of C_6H_6–X complexes, we have made use of the forbidden nature of benzene's $S_1(B_{2u}) \leftarrow S_0(A_{1g})$ transition as a vibronic level indicator of the binding sites taken up by the complexing molecule.[12,14–17] While the S_0–S_1 transition is electric dipole forbidden in benzene, vibrational levels of e_{2g} symmetry can induce intensity in the transition by coupling to the $S_3(E_{1u})$ state whose transition from S_0 is dipole-allowed and very intense (f = 0.88).[22] ν_6, an e_{2g} in-plane ring elongation mode, is first-order allowed, and the 6^1_0 transition is one of the most intense vibronic transitions in the spectrum of free benzene.[23]

Following complexation to a solvent molecule X, the reduced symmetry of the complex may induce intensity in vibronic transitions in benzene which are otherwise forbidden.[11,15–17] In the course of this study, we have developed a more systematic procedure for using these transitions to deduce the symmetry of the complex. Table 1 presents a correlation of symmetry labels from benzene (D_{6h}) to C_6H_6–X complexes of varying reduced symmetries. In the complexes, the solvent molecules induce intensity in new vibronic transitions in benzene by distorting the benzene's electron distribution away from its symmetry in free benzene. The new transitions induced by the solvent thus reflect the over-all symmetry of the complex.

Table 1: Symmetry correlation table for C_6H_6 and C_6H_6–X complexes with reduced symmetry.

D_{6h}	C_{6v}	$C_{3v}(\sigma v)$	$C_{3v}(\sigma d)$	$C_{2v}(z)$	$C_s(\sigma_{zx})$	$C_s(\sigma_{yz})$
A_{1g}	A_1	A_1	A_1	**A_1**	**A′**	**A′**
A_{2g}	A_2	A_2	A_2	**A_2**	**A″**	**A″**
B_{1g}	B_2	A_2	A_1	B_1	**A″**	**A′**
B_{2g}	B_1	A_1	A_2	B_2	**A′**	**A″**
E_{1g}	E_1	**E**	**E**	**$B_1 + B_2$**[b]	**A′ + A″**	**A″ + A′**
E_{2g}[a]	**E_2**	**E**	**E**	$A_1 + A_2$	**A′ + A″**	**A′ + A″**
A_{1u}	A_2	A_2	A_2	**A_2**	**A″**	**A″**
A_{2u}	A_1	A_1	A_1	**A_1**	**A′**	**A′**
B_{1u}	B_1	A_1	A_2	B_2	**A′**	**A″**
B_{2u}	B_2	A_2	A_1	B_1	**A″**	**A′**
E_{1u}	E_1	E	E	**$B_1 + B_2$**	**A′ + A″**	**A′ + A″**
E_{2u}	E_2	E	E	$A_1 + A_2$	**A′ + A″**	**A′ + A″**

[a]Symmetry types in bold-faced type have $S_0(^1A_{1g})$–$S_1(^1B_{2u})$ X^1_0 fundamentals vibronically-allowed in C_6H_6–X complexes via coupling to the E_{1u} state of benzene.
[b]Underlined entries will have X^1_0 fundamentals in C_6H_6–X which are split by virtue of the loss of degeneracy in the vibrational modes of benzene induced by complexation with X.

Table 1 highlights in bold-faced type the symmetries of levels which vibronically couple the S_1 and S_3 states in the reduced-symmetry complexes. In complexes of C_{6v} or C_{3v} symmetry, vibronic coupling is the only mechanism for inducing intensity, since the S_0–S_1 transition remains forbidden. X^1_0 fundamentals in vibrations of e_2 (e)

symmetry will be first-order vibronically coupled to the S_3 state in C_{6v} (C_{3v}). As the symmetry of the complex is reduced to C_{2v}, the S_0–S_1 transition becomes allowed (with x polarization), inducing intensity in the origin transition. At the same time, the doubly degenerate vibrations split, with the transition to one member of the X^1_0 doublet being vibronically allowed, the other both electric dipole and vibronically allowed. Below C_{2v} symmetry, a further increase in the number of allowed and vibronically allowed transitions is predicted.

We will see that in the C_6H_6–$CHCl_3$ complex, the application of the scheme shown in Table 1 allows us to deduce the symmetry of the complex. However, information on the orientation of the solvent molecule within this symmetry type must be gained from other data. One such piece of evidence arises from the accumulated experience of workers investigating a large number of aromatic–X complexes.[12,14–17,24–26] In general, complexes which are hydrogen-bonded to the benzene π cloud produce absorptions which are blue-shifted from those of the parent aromatic. For example, C_6H_6–HCl and $-H_2O$ possess frequency shifts of +125, and +50 cm^{-1}, respectively. Purely dispersive interactions, on the other hand, typically give rise to red-shifted transitions (e.g., C_6H_6–Ar[5] and C_6H_6–CCl_4[11] have transitions shifted by –21 and –68 cm^{-1} from C_6H_6).

A π hydrogen bonding interaction in the complex would also be indicated by efficient fragmentation to $C_6H_6^+$ + X following photoionization. As demonstrated clearly in C_6H_6–HCl,[12,26] the fragmentation of the ionized complex in R2PI results from vertical ionization from the hydrogen-bonded neutral structure to a repulsive part of the ionic potential energy surface resulting from the positive end of the dipole on X initially being oriented toward the newly-created positive charge on the benzene ring.

B. The C_6H_6–$CHCl_3$ Complex

Figure 1 presents a laser-induced fluorescence excitation scan in the region near the 6^1_0 transition of C_6H_6. Dominating the spectrum is a transition blue-shifted from benzene's by 178 cm^{-1}. A short progression with spacing 25 cm^{-1} is also observed which scales in intensity with the main peak under all conditions. There is little interference from benzene transitions in the region, aside from a weak transition at +235 cm^{-1} (marked by a B). The narrow peaks marked by arrows in the figure are due to higher clusters whose assignment will be addressed later.

A one-color R2PI spectrum over the same 6^1_0 region monitoring the $[C_6H_6$–$CHCl_3]^+$ and $[C_6H_6]^+$ mass channels is shown in Figure 2. The +178 cm^{-1} peak and the progression built on it dominate the spectra from both mass channels with no corresponding feature in the 1 : 2 mass channel. The spectrum in the 1 : 1 mass channel shows some interference to the red. Concentration studies indicate that these transitions are likely due to the 1 : 2 cluster, as discussed in the next section. We thus assign the +178, 205, and 231 cm^{-1} transitions to the C_6H_6–$CHCl_3$ complex. The blue shift of these transitions relative to benzene is greater than any other C_6H_6–X complex so far

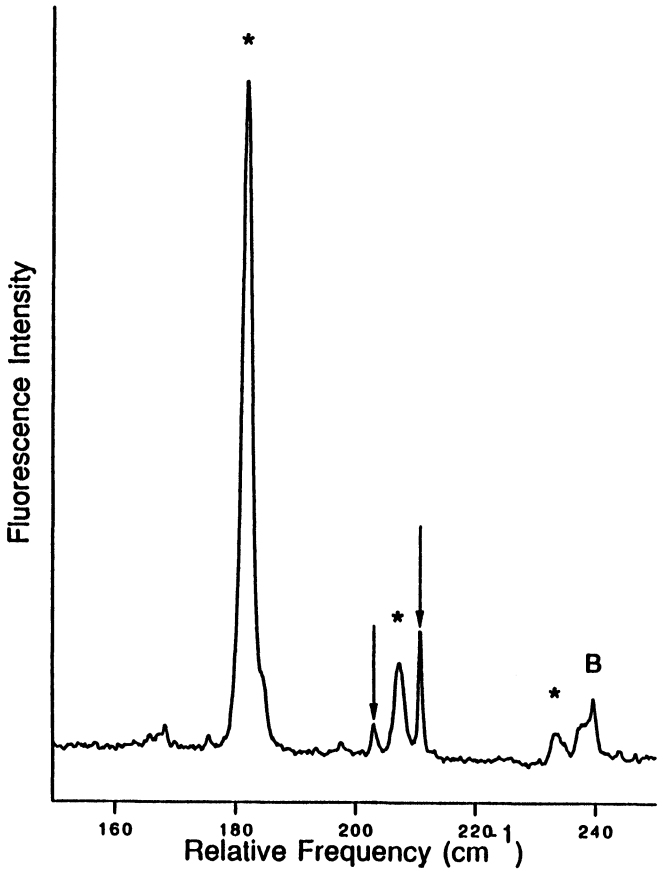

Figure 1 Laser-induced fluorescence excitation scan in the region of the 6^1_0 transition of C_6H_6–$CHCl_3$. The frequency scale is relative to the 6^1_0 transition of free benzene. The peaks marked by an asterisk have been assigned to C_6H_6–$CHCl_3$, a weak benzene transition is marked by a 'B', and two transitions due to higher clusters are marked with arrows. Expansion conditions employ 0.5% C_6H_6, 0.5% $CHCl_3$ at a total pressure of 3 bar.

studied. In addition, the complex undergoes fragmentation with 90–95% efficiency to $C_6H_6^+$ + $CHCl_3$ following one-color photoionization through 6^1_0, even under unfocussed laser conditions following extrapolation to zero laser power.

The large intensity of the 6^1_0 transition of C_6H_6–$CHCl_3$ makes it possible to search with good sensitivity for the corresponding 0^0_0 transition. This transition is not observed, with an upper bound on its intensity of 0.1% of the 6^1_0 transition. Etalon scans of the 6^1_0 transition show no evidence of splitting of the 6^1_0 transition.

Despite not being able to observe the origin transition, the 16^1_0 transition of the complex is observed (Figure 3) with an intensity about 4% of the 6^1_0 transition. ν_{16} is an e_{2u} vibration in benzene, and its 16^1_0 fundamental is forbidden in the isolated

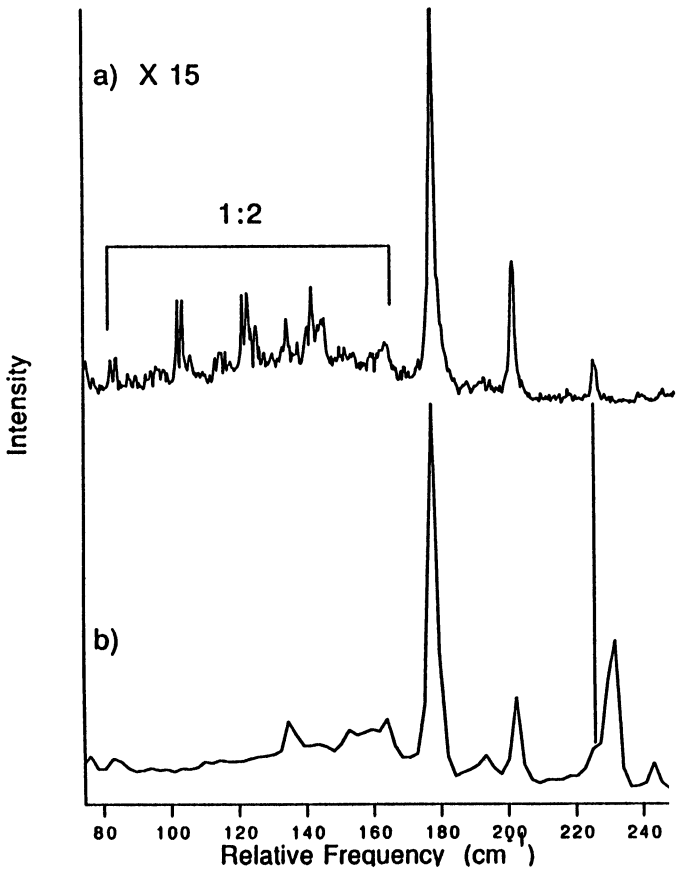

Figure 2 R2PI scans of the 6^1_0 region monitoring a) $[C_6H_6{-}CHCl_3]^+$ and b) $[C_6H_6]^+$ mass channels. The scan in a) is at a 15 times higher sensitivity, indicating extensive fragmentation following photoionization in one-color R2PI. Transitions tentatively assigned to $C_6H_6{-}(CHCl_3)_2$ are marked in the figure. Scan b) was taken at a lower spectral resolution.

molecule. The S_1 frequency of ν_{16} in the complex is unchanged from its value in the free molecule (+238 cm^{-1}). No splitting can be resolved in the transition.

Based on this vibronic level data, which is summarized in Table 2, a C_{6v} or C_{3v} structure is deduced for the $C_6H_6{-}CHCl_3$ complex from Table 1. Given the symmetry of the $CHCl_3$ molecule, the only allowable choice for a rigid complex is C_{3v}, placing the $CHCl_3$ on the six-fold axis of benzene. Both the large blue shift of its absorption relative to benzene and the efficient fragmentation of the complex following photoionization point to a hydrogen-bonded orientation for the $CHCl_3$ molecule in which the hydrogen points in toward the benzene ring.

The vibronic level data of Table 2 cannot rule out non-rigidity in the complex. For instance, the lack of an origin transition could also be produced by an off-axis structure which is capable of free internal rotation about the six-fold axis with an internally-rotationally averaged structure which retains benzene's six-fold symmetry.

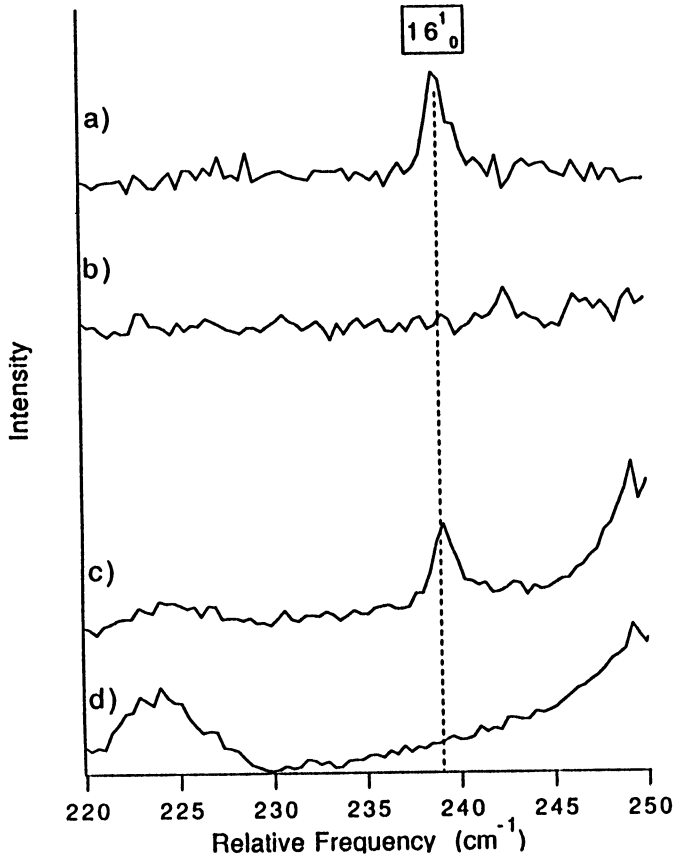

Figure 3 R2PI scan in the 16^1_0 region monitoring a) $[C_6H_6–CHCl_3]^+$ with $CHCl_3$ present, b) $[C_6H_6–CHCl_3]^+$ without $CHCl_3$ present, c) $[C_6H_6]^+$ with $CHCl_3$ present, and d) $[C_6H_6]^+$ without $CHCl_3$ present. Scans a) and b) were recorded at 15 times higher sensitivity than those in c) and d). The 16^1_0 transition observed in the complex is forbidden in C_6H_6.

Table 2: Vibronic level features of $C_6H_6–(CHCl_3)_n$ Clusters

Cluster size	*Freq. shift* (cm^{-1})	*Fragment Ratio*	$0^0_0/6^1_0$ *Intensity*	6^1_0 *splitting* (cm^{-1})	$16^1_0/6^1_0$ *Intensity*	16^1_0 *splitting* (cm^{-1})	*Structure*	*Binding Energy* (cm^{-1})
1 : 1	+178	15 : 1	<0.1%	None	4%	None	C_{3v}	(1620)–2024
1 : 2	+84	>40 : 1	7%	1.5	???	???	"Same side of ring(?)"	???

Alternatively, even if the $CHCl_3$ molecule is on the six-fold axis, it may still be capable of internal rotation of the chlorine atoms about the C–H bond axis. However, the small internal rotation constant of the $CHCl_3$ molecule (c.f. that in H_2O, for instance)[14] means that barriers to internal rotation of only a few wavenumbers would

effectively localize the chlorine atoms. The splitings induced in the spectrum by internal rotation are too small to be observed in the present study, justifying treatment as a C_{3v} hydrogen-bonded structure at our resolution.

Dispersed fluorescence (DFL) scans from the 6^1, $6^1 1^1$, and $6^1 1^2$ levels are shown in Figures 4–6, respectively. In Figure 4a, the DFL scan of 6^1 in free benzene is shown for comparison to 6^1 in the complex. At 6^1, the fluorescence reflects the same vibronic state character as that carrying the oscillator strength in absorption, indicating that state mixing at this level of excitation (521 cm^{-1}) is modest. No evidence of dissociation is present in the spectrum. A "shelf" of intensity just to the red of the $6^1_2 1^0_n$ transitions may signal the beginnings of state mixing with intermolecular levels. The fluorescence lifetime of the 6^1 level of the complex is 32 ± 5 nsec compared to 87 nsec for the free molecule.

The comparison of the $6^1 1^1$ DFL scan of the complex (Figure 5b) with the 0^0 scan of free benzene shows a clear resemblance between the two. However, the prominent

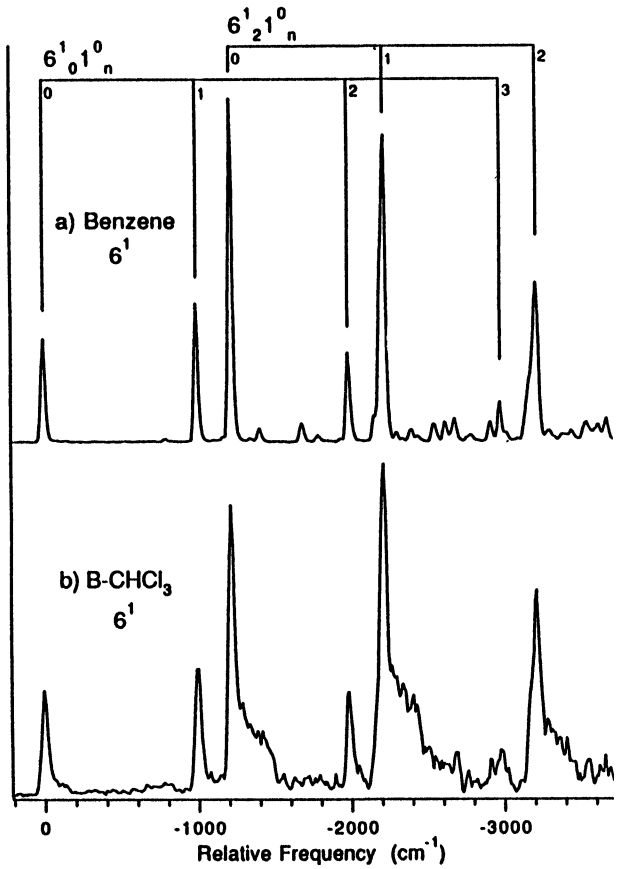

Figure 4 Dispersed fluorescence scan of the emission from the 6^1 level of b) C_6H_6–$CHCl_3$ and from a) C_6H_6 itself for comparison.

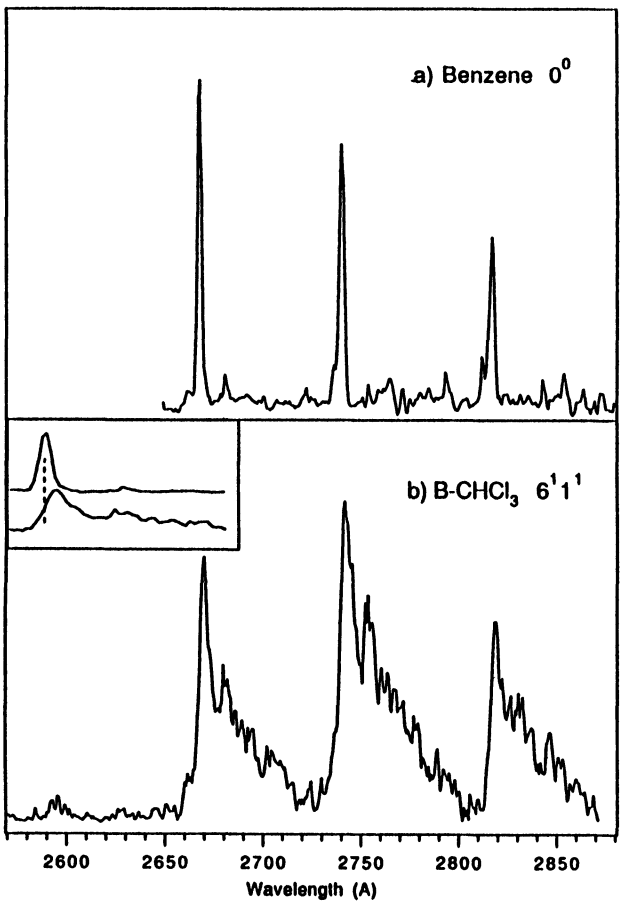

Figure 5 Dispersed fluorescence scan of the emission from the $6^1 1^1$ level of b) C_6H_6–$CHCl_3$ and from a) the 0^0 level C_6H_6 for comparison. The inset in b) shows that even though the peaks are origin-like in appearance, they are not due to the 0^0 of free benzene but rather to fluorescence from background levels built on the origin of type $0^0 vdw^m$ where vdw^m represents excitation of intermolecular (van der Waals') vibrations in the complex.

transitions in the complex's spectrum are red-shifted by about 25 cm^{-1} from that of free benzene (see the inset of Figure 5b) and show satellite structure shaded to the red which is not present in Figure 5a. Furthermore, the fluorescence lifetime of the level is 39 ± 5 nsec, far shorter than the 107 nsec lifetime expected for the 0^0 level of benzene. As a result, no vibrational predissociation occurs on the timescale of the fluorescence. The 0^0-like fluorescence suggests that state mixing between intramolecular and intermolecular modes is extensive at $6^1 1^1$ (1,444 cm^{-1} above the origin), with the predominant character of the emitting modes being $0^0 vdw^m$. Such behavior has been observed previously in several other aromatic–X complexes.[11,27–29] The secondary humps red-shifted from the main peaks by about 160 cm^{-1} are likely $16^1_i 1^0_n vdw^m$ emission.

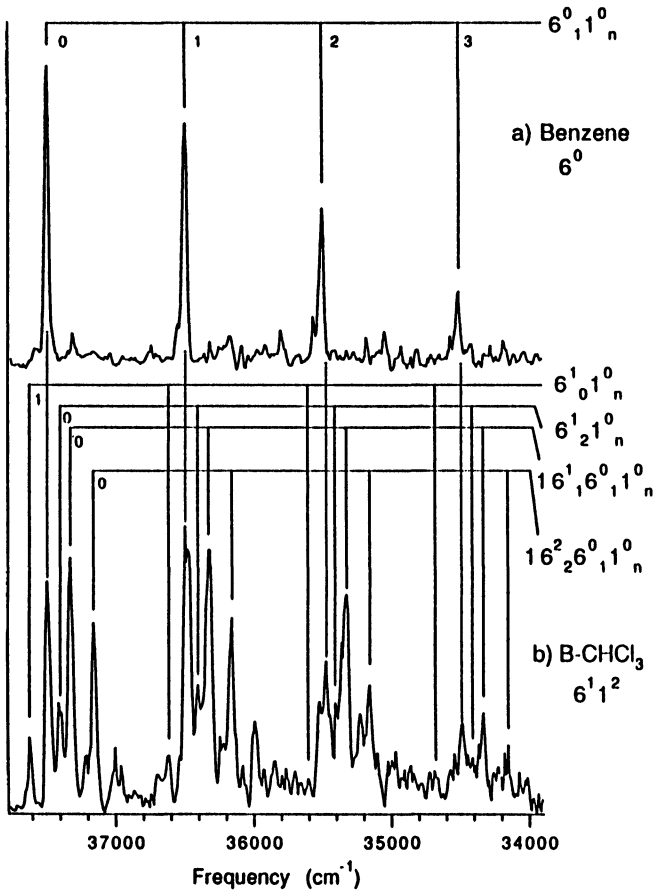

Figure 6 Dispersed fluorescence scan of the emission from the $6^1 1^2$ level of b) C_6H_6–$CHCl_3$ and from a) 0^0 of C_6H_6 for comparison. The emission observed in b) is due to the indicated levels of free C_6H_6 following vibrational predissociation of the complex.

The DFL spectrum from $6^1 1^2$ is from several levels of free benzene following vibrational predissociation of the complex. No remnant of the $0^0 vdw^m$ fluorescence is observed. This is reflected in the longer fluorescence decay time (~80 nsec) of the observed emission. Several benzene products states are present: 0^0, 16^1, 16^2, 6^1. The highest energy of these, 6^1, places a firm upper bound on the excited state binding energy of the complex of $D_0' \leq 1{,}846\ cm^{-1}$. Including the 178 cm^{-1} blue-shift in the absorption leads to a ground state binding energy of $D_0'' \leq 2{,}024\ cm^{-1}$.

C. Larger Clusters

1. C_6H_6–$(CHCl_3)_2$:

Based on the structure of the 1 : 1 complex, one low-energy structure for the 1 : 2 cluster would place a second $CHCl_3$ molecule hydrogen-bonded to the opposite side

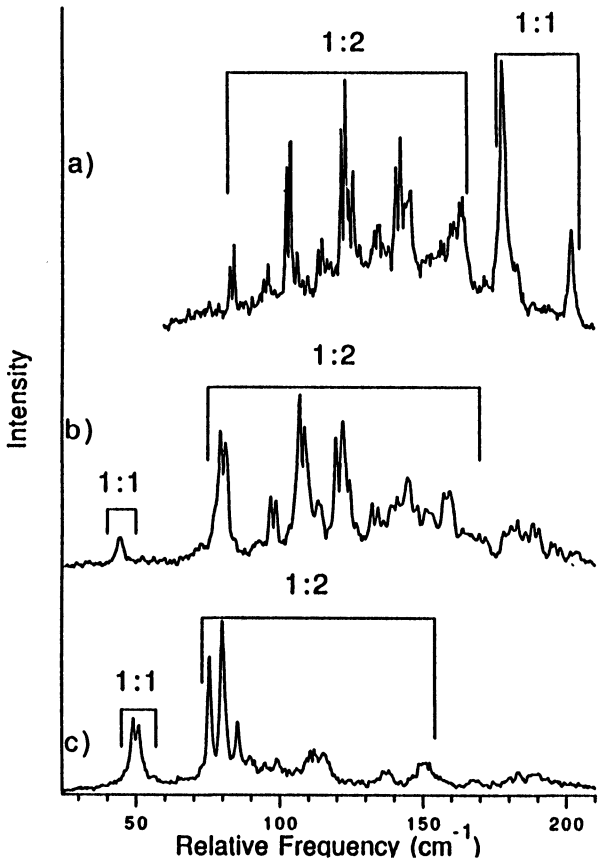

Figure 7 R2PI scans of the 6^1_0 regions comparing the features assigned to a) C_6H_6–$(CHCl_3)_2$ to those of b) C_6H_6–$(CH_3OH)_2$ and c) C_6H_6–$(H_2O)_2$. In each case the spectrum is observed most clearly in the 1 : 1 mass channel.

of the benzene ring. The predicted spectral characteristics for such a cluster structure would include (i) a strong blue-shifted absorption nearly twice the +178 cm^{-1} observed for the 1 : 1 cluster, (ii) a forbidden origin, and (iii) no splitting of the 6^1_0 transition. However, under the range of expansion conditions sampled in the present study, no transitions due to higher clusters were observed to the blue of the 1 : 1 absorptions. Instead, as Figure 7a highlights, a set of transitions is observed in the 1 : 1 mass channel to the red of the 1 : 1 peaks which grow at higher $CHCl_3$ flow relative to the 1 : 1 features. The transitions begin at +84 cm^{-1} and show extensive intermolecular vibrational structure. The 6^1_0 transition and all combination bands built on it are split by 1.5 cm^{-1}. The origin is clearly observed with an intensity 9% that at 6^1_0. We tentatively assign these transitions to the 1 : 2 cluster fragmenting with high efficiency into the 1 : 1 mass channel following photoionization. The vibronic level data is summarized in Table 2.

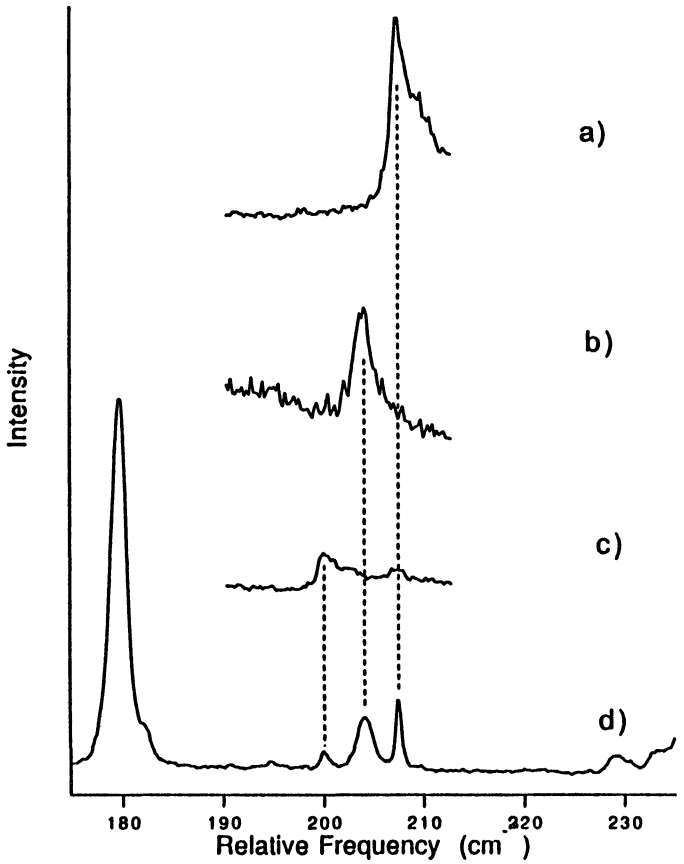

Figure 8 A section of the LIF scan blue of the 6^1_0 transition (d) compared to R2PI scans monitoring a) the $2:3^+$, b) $1:1^+$, and c) $2:2^+$ mass channels, indicating that these peaks are due to higher clusters, probably of composition 2 : 3 and 2 : 4.

A comparison with C_6H_6–$(CH_3OH)_2$ and C_6H_6–$(H_2O)_2$ is given in Figure 7b, c. Note the strong similarities between the spectral characteristics of these 1 : 2 clusters with their intense van der Waals' structure, clear 6^1_0 splitting, strong origin and similar frequency shifts. While the present data provides insufficient evidence for a firm structural determination, the observed transitions are clearly not due to a structure in which the second $CHCl_3$ attaches along the six-fold axis on the opposite side of benzene. Furthermore, the similarities with C_6H_6–$(CH_3OH)_2$ and C_6H_6–$(H_2O)_2$ suggest a similar "same side of the ring" structure for the C_6H_6–$(CHCl_3)_2$ cluster. It seems likely that this structure is the lowest-energy structure for the cluster by virtue of our inability to observe absorptions due to other structural types. However, a strong kinetic preference for formation of this conformer over the Cl_3CH–C_6H_6–$HCCl_3$ conformer cannot be ruled out categorically.

2. The 2 : n Clusters:

Figure 8d reproduces a portion of the fluorescence excitation scan from Figure 1 in the 6^1_0 region of the C_6H_6–$CHCl_3$ complex. As pointed out earlier, this spectrum is complicated by the presence of transitions due to larger clusters. In order to identify the carriers of these transitions, R2PI spectra have been recorded in this region under a wide range of expansion conditions while monitoring an array of mass channels for larger clusters. As Figure 8a, c reveal, the transitions in question appear in the $2 : 2^+$ and $2 : 3^+$ mass channels. Given the efficient fragmentation of even the 1 : 1 cluster by loss of a $CHCl_3$ molecule, it seems likely that these absorptions are due to the 2 : 3 and 2 : 4 clusters, respectively.

It is noteworthy that these transitions are associated, not with 6^1_0, but with 1^1_0, with *red-shifts* of –197 and –204 cm^{-1} from the parent transition. This has been confirmed by scans such as those shown in Figure 9 which identify the corresponding red-shifted transitions associated with the origin, 6^1_0, and 1^1_0. The transitions built on $6^1_0 1^1_0$ and 1^2_0 have also been identified. As shown in Figure 9b, the –197 and –204 cm^{-1} transitions are split at 6^1_0 by 2.2 and 2.4 cm^{-1}, respectively, and are red-shifted slightly from their positions relative to free benzene.

Given the uncertainty in the assignment of cluster size and the presence of (at least) two C_6H_6 molecules in the cluster, the vibronic level data at hand provide no trustworthy structural deductions. Nevertheless, that any $(C_6H_6)_m$–$(CHCl_3)_n$ clusters would have such a large red shift given the large blue shift of the 1 : 1 complex points to significant structural differences in the interactions of benzene and $CHCl_3$ in these clusters, providing fertile ground for further study.

IV. DISCUSSION

The major deductions of this work center on the C_6H_6–$CHCl_3$ complex. In this case, the vibronic level data indicate a structure for the complex in which $CHCl_3$ is on the six-fold axis of benzene, "hydrogen-bonded" to benzene's π cloud. It is not often that the structure of a complex can be deduced with good certainty based solely on vibronic level data. However, the simple, benzene-specific scheme developed in Table 1 and applied to C_6H_6–$CHCl_3$ makes use of symmetry arguments to deduce its point group with little ambiguity. Given the number of C_6H_6–X complexes which have been studied in some detail, it is instructive to review their spectral features using these methods. To that end, Table 3 and Figure 10 summarize the spectral characteristics of several C_6H_6–X complexes with the polar solvents $CHCl_3$, HCl, and H_2O, and with the non-polar solvents C_2H_2 and CCl_4.

As we have seen, in C_6H_6–$CHCl_3$, the lack of an S_0–S_1 origin, the presence of a 16^1_0 transition, and no splitting of the degenerate 6^1 or 16^1 levels predicts a C_{3v} structure for the complex, as shown schematically in Figure 10.

The diatomic HCl provides another clear, testable example of the vibronic level methods since C_6H_6–HCl is known from the microwave studies of Read et al.[13a] and

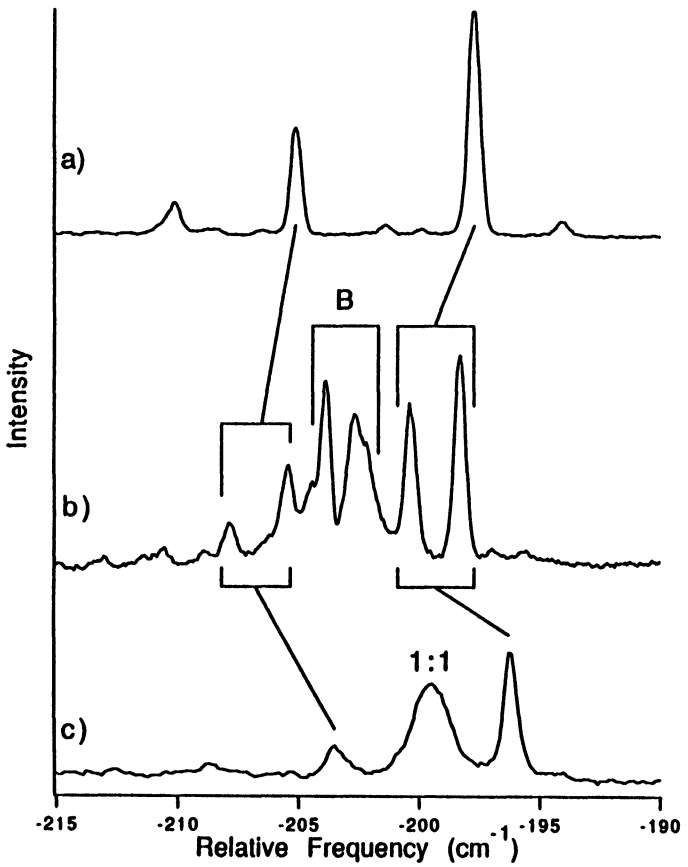

Figure 9 LIF excitation scans of the a) 0^0_0, b) 6^1_0, and c) 1^1_0 transitions of the red-shifted peaks tentatively assigned to the 2 : 3 and 2 : 4 clusters. The zero of the relative frequency scale is the corresponding transitions in free C_6H_6. The transition marked by a 'B' is $6^0_1 1^0_1$ hot band of C_6H_6 while the transition marked 1 : 1 is the van der Waals' stretch fundamental of C_6H_6–$CHCl_3$ built on 6^1_0. The transitions at 6^1_0 are split by 2.0 cm^{-1}.

Balle et al.[13b] to be C_{6v} symmetry with HCl hydrogen-bonded to benzene. R2PI spectra by our group have confirmed this structure and extended it to the S_1 state by the rotational band contour fitting of the 6^1_0 transition.[12] At the same time, the vibronic level data for the complex (Table 3) are uniquely consistent with this structure. As Figure 10 shows in schematic form, no S_0–S_1 origin is observed for the complex. Neither is the 6^1_0 transition of C_6H_6 measurably split by HCl. A search was never carried out for the 16^1_0 transition, but it is predicted to be weakly allowed and unsplit, as it was in C_6H_6–$CHCl_3$. From Table 3, a C_{6v} or C_{3v} structure is deduced, with the C_{6v} structure being consistent with a diatomic's attachment to benzene.

Similarly, one of the two conformers[10,30] of C_6H_6–C_2H_2 possesses no origin (<0.1% of 6^1_0), a weak 16^1_0 transition (2% of 6^1_0), and no splitting at 6^1 or 16^1, again pointing to a C_{6v} structure with the C_2H_2 center-of-mass on the six-fold axis. In this case, it

Table 3: Vibronic Level Probes of C_6H_6–X Structures

C_6H_6 Partner	*Freq. shift (cm^{-1})*	*Fragment Ratio*	*$0^0_0/6^1_0$ Intensity*	*6^1_0 splitting (cm^{-1})*	*$16^1_0/6^1_0$ Intensity*	*16^1_0 splitting (cm^{-1})*	*Structure*	*Binding Energy (cm^{-1})*
$CHCl_3$	+178	15 : 1	<0.1%	None	4%	None	C_{3v}	(1620)–2024
HCl[a]	+125	50 : 1	<1%	None	???	???	C_{6v}	(645)–1330
H_2O[b]	+55	14 : 1	<0.1%	Internal rotation	???	???	G_{24}	(570)–970
C_2H_2[c]	+138	15 : 1	<0.1%	None	2%	None	C_{6v}	(520)–730
CCl_4[d]	–68	2 : 1	18%	2.6	2%	Yes	C_{2v} or lower	(850)–1140

[a]Ref. 12.
[b]Ref. 14.
[c]Previous data of Carrasquillo et al. (Ref. 10) have shown that two conformers of C_6H_6–C_2H_2 exist, one with C_{6v} structure (shown in the table), the other with C_s structure.
[d]Ref. 11.

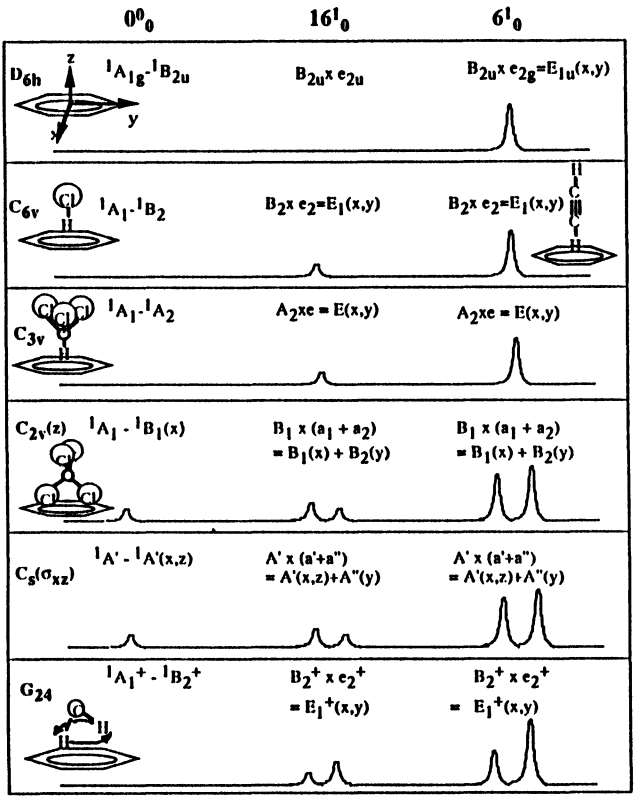

Figure 10 A schematic presentation of the single vibronic level $S_1 \leftarrow S_0$ spectra predicted for C_6H_6–X complexes as a function of their symmetry.

is not clear from the vibronic level alone whether the acetylene molecule lies perpendicular to the benzene ring, or freely internally rotates in a parallel orientation.

The spectral features of the C_6H_6–CCl_4 complex (Table 3) have been detailed in a recent paper by Gotch et al.[11] In this case, the origin is strongly induced by complexation, with intensity 18% of that at 6^1_0. The 16^1_0 and 6^1_0 transitions are both observed and are split by about 2.5 cm^{-1}. The members of the 16^1_0 and 6^1_0 doublets are of unequal intensity. As Figure 10 shows, the complex is deduced on this basis to have at most a $C_{2v}(z)$ structure.[31] For a complex of this symmetry, the S_0–S_1 transition is dipole allowed with transition moment along the x axis, producing an origin transition. The e_{2g} and e_{2u} vibrations split to $a_1 + a_2$, with the 'a_2' component being vibronically induced while the 'a_1' level has both dipole allowed and vibronically induced intensity contributions. It should be noted that the deduction of References 11 that the complex must be at most C_s in symmetry is incorrect due to an error in the symmetry of ν_{16}.

As a final example, the C_6H_6–H_2O complex addresses the effect of non-rigidity on the vibronic level data.[14] As shown in Table 3, the C_6H_6–H_2O complex possesses no origin (with intensity <0.1% of 6^1_0), but its 6^1_0 transition is split to an unequal intensity doublet with 1.6 cm^{-1} splitting. Taken as a rigid structure, these two features are incompatible with one another. However, the doubling at 6^1_0 is removed when HDO is substituted for H_2O. A partial fit of the rotational structure for the complex is accomplished after allowing for non-rigidity of the H_2O molecule involving internal rotation about the six-fold axis and exchange of water's hydrogens which produce m = 0, m = ±1 levels with different nuclear spin symmetry (where m is the internal rotation quantum number).[14] If nuclear spin statistics alone dictate intensities, a 3 : 1 ratio for m = 0/m = ±1 is predicted. $\Delta m = 0$ transitions out of m = 0 and m = ±1 lead to a doubling in the 6^1_0 transition, as observed. The high resolution studies of Suzuki, et al.[31] have confirmed and sharpened this picture. In addition, they have shown unambiguously that the water molecule has the hydrogen(s) pointing in to the ring, consistent with the blue-shift and efficient fragmentation observed in our R2PI studies. Thus, the presence of non-rigidity in the complex can lead to anomalous behavior even at the vibronic level which is a clue to its presence. This same non-rigidity significantly complicates the rotational structure and its analysis in a high resolution scan.

Some final comments on the π hydrogen bond are in order. Table 3 and Figure 10 include three structurally well-characterized π hydrogen-bonded complexes: C_6H_6–HCl, C_6H_6–$CHCl_3$, and C_6H_6–H_2O. $CHCl_3$ and HCl have a single hydrogen-bonding hydrogen while water has two such hydrogens. In all three complexes, the vibrationally-averaged structure for the complex retains the six-fold symmetry of benzene. In the case of C_6H_6–HCl, the microwave studies[12] indicate that while the chlorine atom is on the six-fold axis, the hydrogen takes up a vibrationally-averaged structure which is 20 degrees off the six-fold axis. The microwave data is not able to distinguish between a global minimum in the potential energy surface (PES) for hydrogen on the six-fold axis and a surface with a small barrier at $\theta = 0$. However, molecular mechanics on clusters (MMC) calculations on C_6H_6–HCl show a single minimum with the HCl hydrogen on the axis, indicating a strong orientation

preference for H down.[18] Even in this case, a vibrationally-averaged off-axis orientation results from the heavier weighting of off-axis structures in the degenerate torsional wave functions.

In the same way, the $CHCl_3$ molecule appears to have a clear orientational preference for hydrogen down, both from its large blue-shift and efficient fragmentation of the photoionized complex. The present data cannot determine whether the global minimum in the PES is on the six-fold axis. Energy minimization calculations on the complex using an intermolecular potential developed by Severance and Jorgenson predict a minimum for H on the six-fold axis.[32] Once again, heavier off-axis weighting of the degenerate intermolecular torsional modes will lead to a vibrationally-averaged structure which is somewhat off the six-fold axis. Thus, in both C_6H_6–HCl and C_6H_6–$CHCl_3$ the π hydrogen bond differs structurally from a conventional bond primarily in providing a highly symmetric potential for motion of H off the bond axis which leads to a vibrationally-averaged structure for the hydrogen bond with a slight tilt away from $\theta = 0$.

By contrast, in C_6H_6–H_2O, the two hydrogen-bonding hydrogens on H_2O interact with the delocalized π cloud to produce significant floppiness in the complex. Internal rotation of the water molecule about the six-fold axis and exchange of hydrogens is allowed even at the zero point level. MMC calculations[18] predict a barrier to internal rotation of the water molecule about the six-fold axis of benzene of less than 2 cm^{-1}. They show further that the water molecule can tumble about 1.6 Å across the face of the benzene ring by swapping the hydrogen which is bonded to the ring with almost no change in the total binding energy to the ring. Thus, the net effect of water's two hydrogen bonding hydrogens on its interactions with benzene's delocalized π cloud is to produce an intermolecular potential energy surface which supports large-amplitude motions of water about a nominally hydrogen-bonded configuration. This ability of the water molecule to re-orient on the benzene π cloud with little cost in energy is thus quite different than a traditional X···HY hydrogen bond in which the hydrogen bond is localized between two electronegative atoms X and Y.

The strengths of the π hydrogen-bonds in C_6H_6–HCl, –$CHCl_3$, and –H_2O show a considerable range, but appear to be about one-third to two-thirds the strength of an X···HY hydrogen bond. The upper bounds on the binding energies listed in Table 3 are firm since they are based on detection of emission from free benzene following vibrational predissociation of the S_1 complexes. Tentative lower bounds are given in parentheses, where the assumption is made that a lack of predissociation from an S_1 vibronic level on the time-scale of the fluorescence indicates that the complex has been excited below the dissociation threshold. If an ordering of the upper bounds for the complex can serve as a rough guide to binding strengths, it seems that $D_0(C_6H_6\text{–}CHCl_3) > D_0(C_6H_6\text{–}HCl) > D_0(C_6H_6\text{–}H_2O)$. This ordering reflects, not the dipole moments of the molecules (1.01 D, 1.08 D, and 1.85 D, respectively), but rather their polarizabilities (8.50, 2.63, and 1.48×10^{-24} cm^3, respectively). The ordering also is in keeping with the ordering of blue-shifts of the S_0–S_1 absorptions relative to benzene (+178 > +125 > +55 cm^{-1}) which we have taken as a rough indicator of the strength of π hydrogen bonding. The magnitude of the binding in C_6H_6–$CHCl_3$ ($4.6 \leq D_0'' \leq 5.8$ kcal/mol) is somewhat larger than the binding

calculated by the intermolecular OPLS potential of Jorgenson and co-workers ($D_e'' = 4.3$ kcal/mol).[32] Whether this difference reflects a kinetic shift in the experimental data or a deficiency in the intermolecular potential is still an open question. Despite this, a binding energy of this magnitude provides additional support for solution phase studies whose interpretation hinges on the formation of a well-defined 1 : 1 C_6H_6–$CHCl_3$ complex in solution.[19,20]

Finally, the strikingly different spectral characteristics of 1 : 1 (large blue shift, no origin) and 2 : n (large red shift, intense origin) clusters suggests that even in solution it may be possible to choose ultraviolet excitation wavelengths which select certain solvent orientations around solute molecule(s).[33]

Acknowledgements

Acknowledgement is made to to the National Science Foundation (CHE–9108376) and to the Donors of the Petroleum Research Fund, administered by the American Chemical Society, for their support of this research.

References

1. R. L. Whetten and M. Y. Hahn in *Studies in Physical and Theoretical Chemistry.*, Vol. 68, *Atomic and Molecular Clusters*, ed. E. R. Bernstein (Elsevier, Amsteradam, 1990) p. 765.
2. M. Y. Hahn and R. L. Whetten. *Phys. Rev. Lett.*, 61, 1190 (1988).
3. Th. Weber and H. J. Neusser. *J. Chem. Phys.*, **94**, 7689 (1991).
4. W. Scherzer, H. L. Selzle, and E. W. Schlag. *Chem. Phys. Lett.*, **195**, 11 (1992).
5. M. Schmidt, M. Mons, and J. LeCalve. *Chem. Phys. Lett.*, **177**, 371 (1991); M. Schmidt, J. LeCalve, and M. Mons. *J. Chem. Phys.*, (in press).
6. J. A. Menapace and E. R. Bernstein. *J. Am. Chem. Soc.*, **91**, 2533 (1987).
7. E. R. Bernstein. in *Studies in Physical and Theoretical Chemistry.*, Vol. 68, *Atomic and Molecular Clusters.*, ed. E. R. Bernstein (Elsevier, Amsterdam, 1990) p. 551 and references therein.
8. R. Nowak, J. A. Menapace, and E. R. Bernstein. *J. Chem. Phys.*, **89**, 1309 (1988).
9. M. Schauer and E. R. Bernstein. *J. Chem. Phys.*, **82**, 726 (1985).
10. E. Carrasquillo M., T. S. Zwier, and D. H. Levy. *J. Chem. Phys.*, **83**, 4990 (1985).
11. A. J. Gotch, A. W. Garrett, and T. S. Zwier. *J. Phys. Chem.*, **95**, 9699 (1991).
12. A. J. Gotch and T. S. Zwier. *J. Chem. Phys.*, **93**, 6977 (1990).
13. a) W. G. Read, E. J. Campbell, and G. Henderson. *J. Chem. Phys.*, **78**, 3501 (1983); b) T. J. Balle, E. J. Campbell, M. R. Keenan, and W. H. Flygare. *J. Chem. Phys.*, **72**, 922 (1980).
14. A. J. Gotch, A. W. Garrett, D. L. Severance and T. S. Zwier. *Chem. Phys. Lett.*, **178**, 121 (1991); A. J. Gotch and T. S. Zwier. *J. Chem. Phys.*, **96**, 3388 (1992).
15. A. W. Garrett and T. S. Zwier. *J. Chem. Phys.*, **96**, 3402 (1992).
16. A. W. Garrett, D. L. Severance and T. S. Zwier. *J. Chem. Phys.*, **96**, 7245 (1992).
17. A. W. Garrett and T. S. Zwier. *J. Phys. Chem.*, **96**, 9710 (1992).
18. J. D. Augspurger, C. E. Dykstra, and T. S. Zwier. *J. Phys. Chem.*, **96**, 7252 (1992).
19. K. Sato and A. Nishioka, Bull. *Chem. Soc.*, Japan, **44**, 1506 (1971).
20. R. Mierzecki. *Rocz. Chem.*, **46**, 1375 (1972).
21. L. H. Spangler, R. D. van Zee and T. S. Zwier. *J. Phys. Chem.*, **91**, 2782 (1987).
22. G. W. Robinson. *J. Chem. Phys.*, **46**, 572 (1967).
23. A. E. W. Knight, C. S. Parmenter, and M. W. Schuyler. *J. Am. Chem. Soc.*, **97**, 1993 (1975).
24. M. Ito. *J. Mol. Struct.*, **177**, 173 (1988); T. Ebata, M. Furukawa, T. Suzuki, and M. Ito. *J. Opt. Soc. Am.*, B **7**, 1890 (1990).
25. K. Fuke and K. Kaya. *Chem. Phys. Lett.*, **94**, 97 (1983).
26. J. R. Gord, A. W. Garrett, R. E. Bandy and T. S. Zwier. *Chem. Phys. Lett.*, **171**, 443 (1990).
27. C. A. Haynam, D. V. Brumbaugh and D. H. Levy. *J. Chem. Phys.*, **79**, 1581 (1983).
28. D. O. DeHaan and T. S. Zwier. *J. Chem. Phys.*, **90**, 1460 (1989).

29. E. J. Bieske, A. S. Uichanco, M. W. Rainbird and A. E. W. Knight. *J. Chem. Phys.*, **94**, 7029 (1991).
30. A second conformer of C_6H_6–C_2H_2 has been deduced to have a C_s structure from rotational band contour fitting (References 10). This conformer has not been included in this discussion because of its unusual C_2H_2 concentration dependence and fragmentation, which are also consistent with a 1 : 2 cluster.
31. S. Suzuki, P. G. Green, R. E. Bumgarner, S. Dasgupta, W. A. Goddard III and G. A. Blake, Science, **257**, 942 (1992).
32. D. Severance and T. S. Zwier, unpublished results.
33. M. Koyanagi and Y. Kanda. *Spectrochim. Acta.*, **20**, 993 (1964).